



Original article

Discovery of potent anticancer agent **HJC0416**, an orally bioavailable small molecule inhibitor of signal transducer and activator of transcription 3 (STAT3)



Haijun Chen ^{a, c, 1}, Zhengduo Yang ^{b, 1}, Chunyong Ding ^a, Ailian Xiong ^b, Christopher Wild ^a, Lili Wang ^b, Na Ye ^a, Guoshuai Cai ^b, Rudolfo M. Flores ^a, Ye Ding ^a, Qiang Shen ^{b, *}, Jia Zhou ^{a, *}

^a Chemical Biology Program, Department of Pharmacology and Toxicology, University of Texas Medical Branch, Galveston, TX 77555, United States

^b Department of Clinical Cancer Prevention, Division of Cancer Prevention and Population Sciences, The University of Texas M.D. Anderson Cancer Center, Houston, TX 77030, United States

^c College of Chemistry and Chemical Engineering, Fuzhou University, Fuzhou, Fujian 350002, China

ARTICLE INFO

Article history:

Received 10 March 2014

Received in revised form

15 May 2014

Accepted 21 May 2014

Available online 22 May 2014

Keywords:

STAT3 inhibitors

Oral bioavailability

Breast cancer

Pancreatic cancer

Anticancer agents

ABSTRACT

In a continuing effort to develop orally bioavailable small-molecule STAT3 inhibitors as potential therapeutic agents for human cancer, a series of novel diversified analogues based on our identified lead compound **HJC0149** (**1**) (5-chloro-*N*-(1,1-dioxo-1*H*-1λ⁶-benzo[*b*]thiophen-6-yl)-2-hydroxybenzamide, *Eur. J. Med. Chem.* **2013**, 62, 498–507) have been rationally designed, synthesized, and pharmacologically evaluated. Molecular docking studies and biological characterization supported our earlier findings that the *O*-alkylamino-tethered side chain on the hydroxyl group is an effective and essential structural determinant for improving biological activities and druglike properties of these molecules. Compounds with such modifications exhibited potent antiproliferative effects against breast and pancreatic cancer cell lines with IC₅₀ values from low micromolar to nanomolar range. Among them, the newly discovered STAT3 inhibitor **12** (**HJC0416**) displayed an intriguing anticancer profile both *in vitro* and *in vivo* (i.p. & p.o.). More importantly, **HJC0416** is an orally bioavailable anticancer agent as a promising candidate for further development.

© 2014 Elsevier Masson SAS. All rights reserved.

1. Introduction

Signal transducer and activator of transcription 3 (STAT3) is the most studied member of a family of seven proteins (STAT1, 2, 3, 4, 5a, 5b, and 6) that are involved in the regulation of early embryonic development, angiogenesis, immune response, cell proliferation, differentiation, and apoptosis [1–5]. From nearly two decades of research on STAT3, accumulating evidence has demonstrated that STAT3 is hyperactivated in many human tumors and represents an attractive therapeutic target for the treatment of various types of cancer [6–12]. However, despite many years of intensive research devoted to the discovery of small molecules targeting STAT3, only several compounds are in early phase clinical trials, and currently there are no candidates approved for clinical use in oncology

[13–15]. The suitability of the scaffolds and physicochemical properties are most significant issues in promoting a potent agent into clinical trials [16]. Thus, there is an urgent need to develop novel diversified scaffolds, and orally bioavailable drug candidates capable of targeting STAT3 [17].

Our previous work by utilizing fragment-based drug design (FBDD) approach has explored several novel scaffolds targeting STAT3 as potent anticancer agents [18]. The identified drug candidates including **HJC0149** (**1**) with enhanced pharmacological activities and especially drug-like properties may act as advanced chemical leads for further optimization (Fig. 1) [18]. Another previous effort in our laboratories has demonstrated that it is feasible to identify new niclosamide derivatives with improved oral bioavailability through modifications of the hydroxyl group on the phenol ring tethered by an *O*-alkylamino side chain, leading to the identification of **HJC0152** with a similar or significantly higher anticancer potency on proliferation of human breast and pancreatic cancer cells [19]. Pharmacological evaluation revealed that **HJC0152** inhibited STAT3 promoter activity, and increased the expression of

* Corresponding authors.

E-mail addresses: qshen@mdanderson.org (Q. Shen), jizhou@utmb.edu (J. Zhou).

¹ These authors contribute equally to this work.

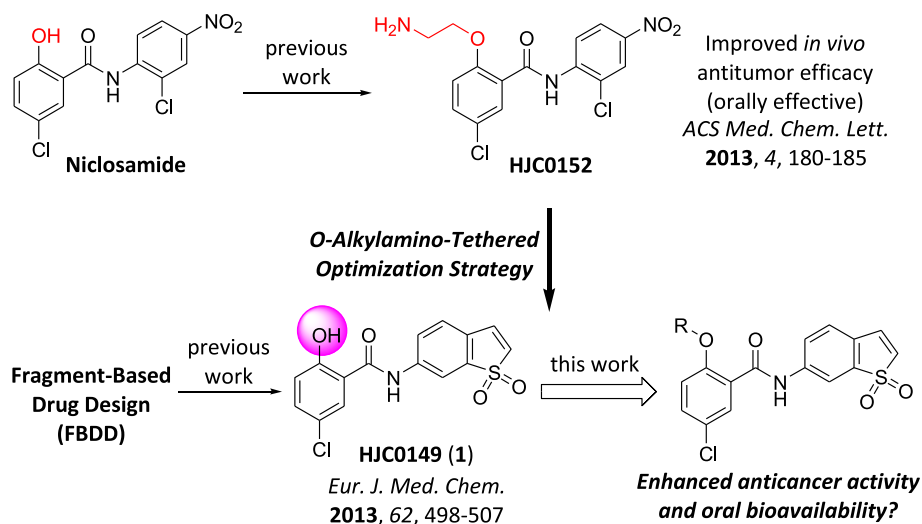


Fig. 1. Previous work and drug design strategy for the current work.

active caspase-3. Further *in vivo* studies in nude mice bearing triple-negative breast tumor xenografts demonstrated that **HJC0152** significantly suppressed tumor growth (both *i.p.* & *p.o.*) [19]. These results suggest that chemical optimization of the hydroxyl group of salicylic amide scaffold in niclosamide may be a viable strategy to develop novel orally bioavailable agents for human cancer therapy.

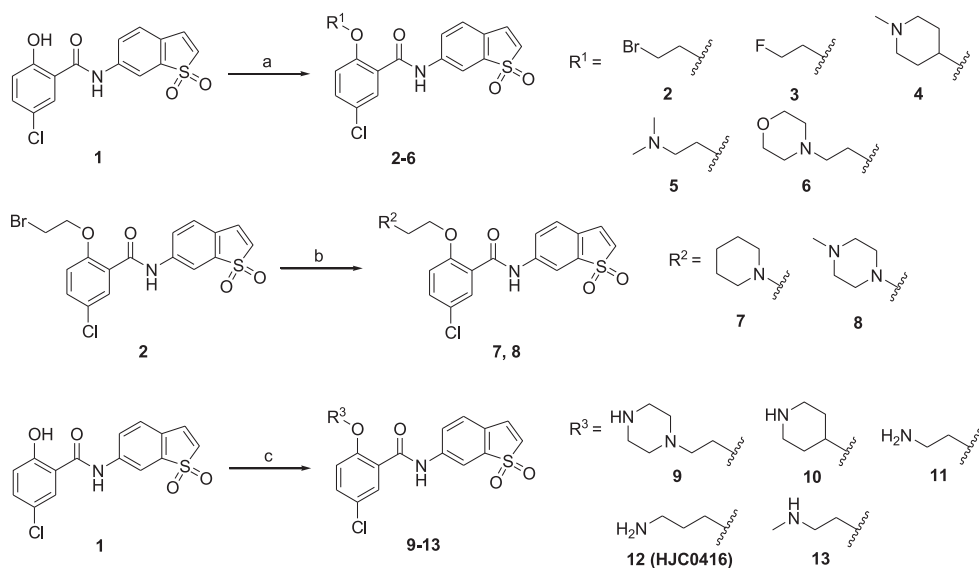
In a continuing effort to develop novel diversified analogues based on the scaffold of lead compound **1**, we directed our chemical optimization involving modification of the hydroxyl group on the phenol ring by introduction of *O*-alkylamino side chains as depicted in Fig. 1. We envisioned that such modifications on the salicylic amide moiety of **1** by utilizing the same strategy might enhance both anticancer potency and oral bioavailability. Herein, we report the lead optimization of compound **1** with a focus on improving

anticancer activity and bioavailability. These studies led to the discovery of an orally efficacious anticancer agent **12 (HJC0416)**, a promising candidate for further drug development.

2. Results and discussion

2.1. Chemistry

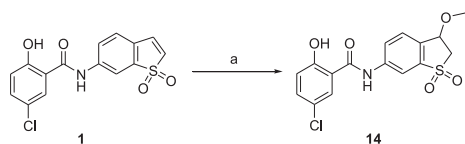
The synthesis of new derivatives based on salicylic amide scaffold with chemical optimization of the hydroxyl group is outlined in Scheme 1. Analogues **2–6** were conveniently prepared by Mitsunobu reaction of the appropriate substituted alcohols with lead compound **1** in 39–77% yields. Alkylation of the bromide intermediate **2** with piperidine or 1-methylpiperazine in the presence of K_2CO_3 and KI in acetone introduced basic functionalities into the



^a Reagents and conditions: (a) R^1OH , Ph_3P , DIAD, THF, rt, 39–77%; (b) R^2H , KI, K_2CO_3 , acetone, reflux, 77–98%; (c) (i) $Boc-R^3OH$, Ph_3P , DIAD, THF, rt; (ii) TFA, CH_2Cl_2 , 0 °C to rt, 40–52% (two steps).

Scheme 1.

molecules providing compounds **7** and **8** in yield of 98% and 77%, respectively. Mitsunobu coupling of lead compound **1** with *N*-Boc-protected amino alcohols followed by the Boc-deprotection with the treatment of TFA afforded analogues **9–13** with diversified *O*-alkylamino side chains in 40–52% yields (two steps). Modification of benzo[*b*]thiophene 1,1-dioxide motif by introducing an ether group to the double bond moiety is shown in Scheme 2. Compound **14** was prepared from **1** by the treatment with methanol and 10% aqueous solution of NaOH in yield of 60% [20].



^a Reagents and conditions: (a) 10% NaOH (aq.), MeOH, H₂O, 0 °C to rt, 60%.

Scheme 2.

2.2. Biology

To explore the structure–activity relationship (SAR) and examine how the substitutions of the moiety groups affected biological activities of newly synthesized analogues, we first evaluated the *in vitro* anticancer effects of compounds **2–14** on the proliferation of breast cancer cell lines MCF-7 (ER-positive) and MDA-MB-231 (ER-negative and triple-negative), as well as two pancreatic cancer cell lines AsPC1 and Panc-1 using MTS assays as described in the Experimental Section. The suitable calculated lipophilicity (cLogP) and topological polar surface area (tPSA) values shown in Table 1 suggest that these newly designed analogues are clearly in good alignment with Lipinski's "Rule of Five" and may have ideal physicochemical properties. Meanwhile, the introduced basic functionalities of the target molecules can form HCl salts to facilitate the aqueous solubility. The capabilities of these new analogues to inhibit the growth of cancer cells are summarized in Table 1. Introduction of an *O*-bromoalkyl group into the lead compound **1** resulted in a dramatic loss of activity, and the derivative **2** displayed no significant antiproliferative effects on all tested cell lines. However, further replacement of the bromo with a hydrophilic amino group regained the antiproliferative effects to a similar or significantly enhanced level in comparison with **1**. For instance, *O*-alkylamino-tethered derivatives **4–13** exhibited promising antiproliferative effects against four cancer cell lines with IC₅₀ values from low micromolar to nanomolar range. Compound **6** with a morpholine moiety showed potent antiproliferative effect against MCF-7 with an IC₅₀ value of 0.49 μM. Compound **12** inhibited the proliferation of both ER-positive, and ER-negative (triple negative) breast cancer cells with IC₅₀ values of 1.76 μM and 1.97 μM, respectively. Intriguingly, compound **12** also displayed a marked antiproliferative effect against pancreatic cancer cell line AsPC1 with an IC₅₀ value of 40 nM. Interestingly, the fluorinated derivative **3** displayed moderate to potent antiproliferative effects against the tested cancer cells, indicating that this compound might be suitable for developing as a potential ¹⁸F-radiolabeled positron emission tomography (PET) imaging agent for human cancer [21]. Modification of benzo[*b*]thiophene 1,1-dioxide motif by introducing an ether group to the double bond moiety has been demonstrated to generally reduce the antiproliferative effects. For example, compound **14** displayed only moderate activity against all the tested cell lines, indicating that benzo[*b*]thiophene 1,1-dioxide is an important pharmacophore for this class of molecules. Therefore, more extensive SAR study based upon the scaffold of compound **14** was not pursued.

Among the newly synthesized analogs, compound **12** was selected for a battery of further *in vitro* and *in vivo* characterizations due to its enhanced antiproliferative effects and druglike properties including the aqueous solubility. To further study the anticancer effects of compound **12** on cell growth, cellular morphological changes were examined in MDA-MB-231 breast cancer cells treated with compound **12** or static for 48 h, under light microscopy. As shown in Fig. 2, like static, **12** significantly inhibited cell growth and induced apoptosis accompanying cellular morphological changes at concentration of 1 μM, 5 μM, and 10 μM, respectively.

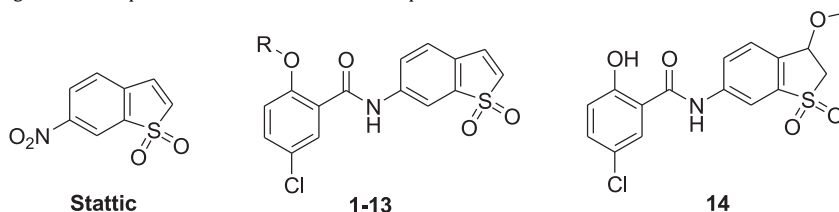
To determine whether compound **12** acts as a potent small-molecule inhibitor of STAT3 activation, we further measured the inhibitory effect on promoter activity using the cell-based transient transfection and dual luciferase reporter assays. MDA-MB-231 cells were pre-treated with static or **12** at the same concentration (5 μM) for 24 h. The STAT3 promoter activity in MDA-MB-231 cells was determined after transient transfecting with pSTAT3-Luc vector. As shown in Fig. 3, treatment with 5 μM of **12** decreased the STAT3 promoter activity in MDA-MB-231 cells by approximately 51%, while static only decreased the STAT3 promoter activity by 39%.

Our previous work and studies from other groups have revealed that compounds with the 1,1-dioxo-1*H*-1λ⁶-benzo[*b*]thiophen-6-yl fragment might interact with STAT3-SH2 domain [18,22]. In an attempt to elucidate the structural basis of the inhibition of STAT3 assembly at the SH2 binding site, it was of interest to determine the possible conformation and binding pose of compound **12** by using AutoDock Vina docking approach [18,23]. As depicted in Fig. 4, the 1,1-dioxo-1*H*-1λ⁶-benzo[*b*]thiophen-6-yl moiety interacted with the pocket of Val637 and Ile659 in a similar fashion as we previously reported [18]. The salicylic amide of compound **1** and compound **12** formed the H-bond with Trp623, while oxygen of 3-aminopropoxy side chain of **12** formed an additional H-bond with Trp623 and terminal amino group formed another H-bond with Glu638. Furthermore, the alkyl chain might have the hydrophobic interactions with Val637. These molecular docking studies could also reasonably explain why the compounds with a hydrophilic amino group or the certain length of the carbon chain might have better anticancer activity. It is worth mentioning that the large pocket formed around Lys591, Glu594, Arg595, Arg609 and Glu612 may be a good starting point for further drug design and structural optimization.

To further investigate the inhibitory activity of compound **12** against STAT3 pathway, we examined STAT3 phosphorylation and expression of the known STAT3 target genes in MDA-MB-231 cell line. The cells were treated with different doses of compound **12** for 12 h, and levels of total STAT3 and phosphorylated STAT3 at Tyr-705 were then examined by Western blot. As shown in Fig. 5, total STAT3 expression in these cells was reduced after treatment with compound **12** or static. Similarly, phosphorylated STAT3 at Tyr-705 is suppressed by compound **12** or static, suggesting that compound **12** has a comparable potency in downregulating STAT3 protein production and phosphorylation at Tyr-705 site. We observed that compound **12** induced cleaved caspase-3 and downregulated cyclin D1 levels in MDA-MB-231 cells. These results suggest that compound **12** inhibits cell cycle progression and promotes apoptosis.

Compound **12** was further evaluated for potential antitumor effects in the MDA-MB-231 triple-negative breast cancer murine xenograft model, and tumor volume was measured daily in intraperitoneal treatment (i.p.) and oral gavage (p.o.) groups. It was found that mice treated with 10 mg/kg of compound **12** via i.p. showed a 67% decrease of tumor volume as compared to the control mice (Fig. 6A). Similarly, we treated the MDA-MB-231 xenograft mice with oral administration of compound **12** and found that the

Table 1
Effects of newly synthesized analogues **2–14** on proliferation of human breast and pancreatic cancer cell lines.



| Compound | R | cLog P ^a | tPSA ^b | IC ₅₀ (μM) ^c | | | |
|----------------|---|---------------------|-------------------|------------------------------------|------------|-------------------|-------|
| | | | | Breast cancer ER-positive | | Pancreatic cancer | |
| | | | | MCF-7 | MDA-MB-231 | | AsPC1 |
| Stattic | | 1.05 | 80.0 | 3.60 | 2.89 | 1.32 | 3.77 |
| 1 | H | 2.88 | 83.5 | 0.91 | 1.64 | 1.92 | 2.34 |
| 2 | | 3.60 | 72.5 | >10 ^d | >10 | ND ^e | ND |
| 3 | | 3.14 | 72.5 | 4.0 | 4.42 | 1.37 | 9.53 |
| 4 | | 3.21 | 75.7 | 3.53 | 2.68 | 1.04 | 1.36 |
| 5 | | 2.74 | 75.7 | 3.5 | 2.69 | 1.14 | 3.38 |
| 6 | | 2.45 | 84.9 | 0.49 | 5.43 | 1.37 | 6.95 |
| 7 | | 3.65 | 75.7 | 3.74 | 2.51 | 1.42 | 1.81 |
| 8 | | 2.54 | 79.0 | 4.08 | 2.86 | 1.07 | 3.01 |
| 9 | | 2.16 | 87.7 | 2.56 | 3.29 | 1.02 | 3.69 |
| 10 | | 2.83 | 84.5 | 4.21 | 2.85 | 1.6 | 4.09 |
| 11 | | 1.91 | 98.5 | 3.47 | 3.12 | 1.05 | 2.25 |
| 12 | | 2.24 | 98.5 | 1.76 | 1.97 | 0.04 | 1.88 |
| 13 | | 2.32 | 84.5 | 3.15 | 3.12 | 2.05 | 3.09 |
| 14 | | 2.43 | 92.7 | 6.07 | 7.05 | 8.46 | 8.39 |

^a Average cLogP: <http://146.107.217.178/lab/alogps/start.html>.

^b tPSA: <http://www.molinspiration.com/cgi-bin/properties>.

^c Breast cancer cell lines: MCF-7 and MDA-MB-231. Pancreatic cancer cell lines: AsPC1 and Panc-1. Software: MasterPlex ReaderFit 2010, MiraiBio, Inc.

^d If a specific compound is given a value >10, it indicates that a specific IC₅₀ cannot be calculated from the data points collected, meaning 'no effect'.

^e ND: not determined.

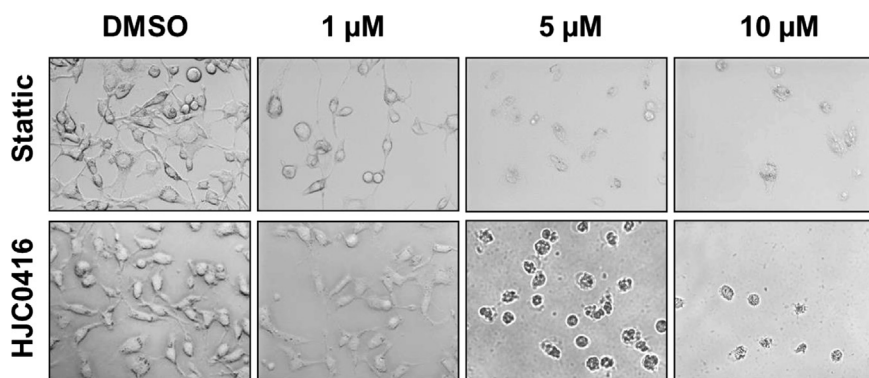


Fig. 2. Effects of **12** (**HJC0416**) and static on cell growth and cellular morphological changes. Exponentially growing MDA-MB-231 breast cancer cells were incubated with **12** or static for 48 h. Cell morphology was evaluated under light microscopy.

growth of xenograft tumors in mice was also significantly reduced at a dose of 100 mg/kg by 46% (Fig. 6B). The i.p. route appeared to have a better reduction of tumor volume, and this observation might be attributed to the efficiency of bioavailability for compound **12**. It is also noteworthy that compound **12** did not show significant signs of toxicity at a dose of 100 mg/kg. These results have demonstrated that compound **12** effectively reduced the tumor growth originated from MDA-MB-231 cells *in vivo* with no significant body weight loss, indicating its low adverse side effects as a drug candidate. Further pharmacokinetic studies and preclinical assessment are under way.

3. Conclusions

In summary, an appropriate modification of the hydroxyl group of salicylic amide scaffold enabled us to expand the scope of the exploration of the series, leading to the identification of several potent STAT3 inhibitors with enhanced anticancer activities and druglike properties. Through the optimization of the lead compound **1**, a novel *O*-alkylamino-tethered derivative **12** has been discovered to exhibit potent antiproliferative effects, inhibit STAT3 promoter activity, and decrease the expression of phosphorylated STAT3. Molecular docking studies support our findings that the *O*-alkylamino side chain on the hydroxyl group of this class of

compounds is an effective and essential structural determinant for improving biological activity and druglikeness. Intriguingly, **12** significantly suppressed MDA-MB-231 xenograft tumor growth *in vivo* (i.p. & p.o.), indicating its great potential as an orally bioavailable anticancer agent. This work together with our previous efforts enabled us to establish a sizable compound library of druglike STAT3 inhibitors with diversified scaffolds and may open new venues for further clinical development of promising candidates for human cancer therapeutic regimens.

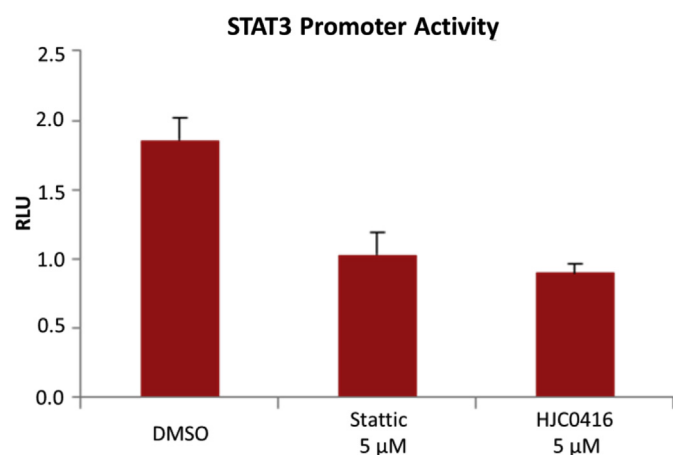


Fig. 3. Compound **12** (**HJC0416**) inhibited the STAT3 mediated luciferase reporter activity in MDA-MB-231 cells. STAT3 promoter activity was measured using dual luciferase assay with a STAT3 reporter. Promoter activity obtained from DMSO-treated MDA-MB-231 cells was used as control. Error bars represent standard deviation of triplicate wells. Representative experiment from at least 3 independent experiments is shown. RLU: relative luciferase unit.

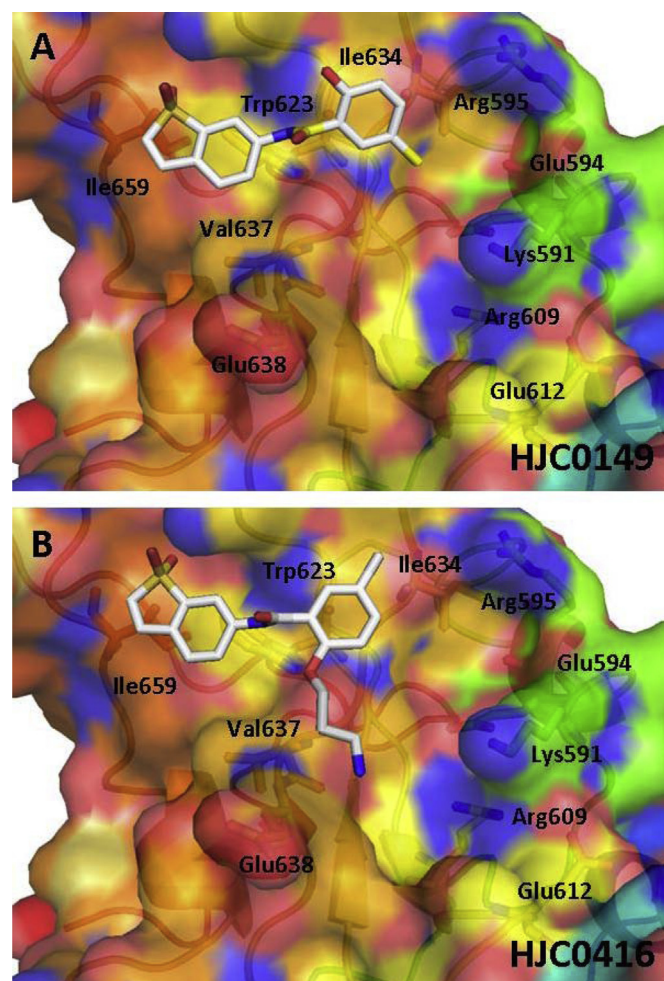


Fig. 4. Predicted binding modes for **HJC0149** (**1**) and **HJC0416** (**12**). The figures were generated using Pymol.

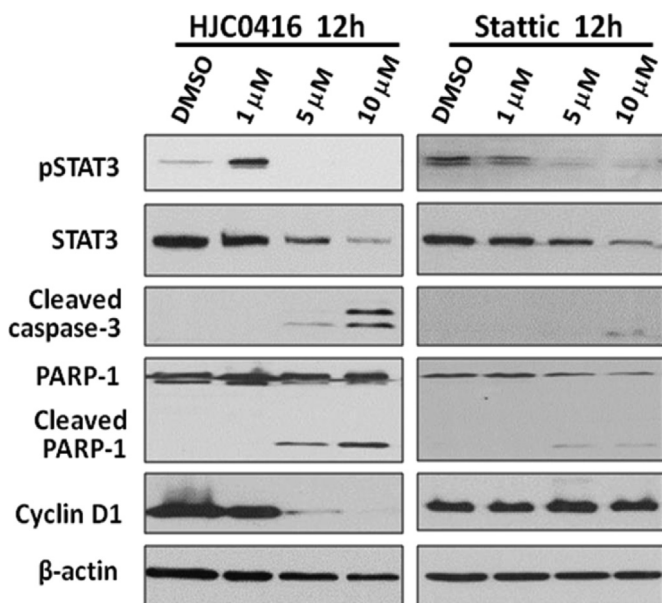


Fig. 5. Western blot analysis of biochemical markers for apoptosis induction and inhibition of STAT3 activity by stattic and compound **12** in the MDA-MB-231 cell line. Cells were treated with stattic or **12** for 12 h, levels of pSTAT3, STAT3, cleaved caspase-3, PARP-1, cleaved PARP-1 and cyclin D1 were probed by specific antibodies. β -actin was used as the loading control.

4. Experimental section

4.1. Chemistry

All commercially available starting materials and solvents were reagent grade, and used without further purification. Reactions were performed under a nitrogen atmosphere in dry glassware with magnetic stirring. Preparative column chromatography was performed using silica gel 60, particle size 0.063–0.200 mm (70–230 mesh, flash). Analytical TLC was carried out employing silica gel 60 F254 plates (Merck, Darmstadt). Visualization of the developed chromatograms was performed with detection by UV (254 nm). NMR spectra were recorded on a Bruker-600 (^1H , 600 MHz; ^{13}C , 150 MHz) spectrometer. ^1H and ^{13}C NMR spectra were recorded with TMS as an internal reference. Chemical shifts

were expressed in ppm, and J values were given in Hz. High-resolution mass spectra (HRMS) were obtained from Thermo Fisher LTQ Orbitrap Elite mass spectrometer. Parameters include the following: Nano ESI spray voltage was 1.8 kV; Capillary temperature was 275 °C and the resolution was 60,000; Ionization was achieved by positive mode. Melting points were measured on a Thermo Scientific Electrothermal Digital Melting Point Apparatus and uncorrected. Purity of final compounds was determined by analytical HPLC, which was carried out on a Shimadzu HPLC system (model: CBM-20A LC-20AD SPD-20A UV/VIS). HPLC analysis conditions: Waters μ Bondapak C18 (300 \times 3.9 mm); flow rate 0.5 mL/min; UV detection at 270 and 254 nm; linear gradient from 30% acetonitrile in water (0.1% TFA) to 100% acetonitrile (0.1% TFA) in 20 min followed by 30 min of the last-named solvent. All biologically evaluated compounds are >95% pure.

4.1.1. 2-(2-Bromoethoxy)-5-chloro-N-(1,1-dioxo-1H-1 λ^6 -benzo[b]thiophen-6-yl)benzamide (**2**)

To a solution of 5-chloro-N-(1,1-dioxo-1H-1 λ^6 -benzo[b]thiophen-6-yl)-2-hydroxybenzamide (**1**, **HJC0149**) [18] (200 mg, 0.6 mmol) and PPh_3 (314 mg, 1.2 mmol) in THF (5 mL) was added 2-bromoethanol (150 mg, 1.2 mmol) and DIAD (218 mg, 1.08 mmol). The mixture was stirred at r.t. for 16 h. The reaction mixture was diluted with EtOAc (100 mL) and extracted with H_2O (40 mL). The organic layer was washed with brine (10 mL), dried with anhydrous Na_2SO_4 , and then concentrated to give the crude product. This residue was purified with silica gel column (Hexane/Acetone = 2/1 to 1/2) to provide **2** (200 mg, 75%) as a yellow solid (mp 235–236 °C). ^1H NMR (600 MHz, $\text{DMSO}-d_6$) δ 10.59 (s, 1H), 8.26 (s, 1H), 7.89 (d, 1H, $J = 7.8$ Hz), 7.70 (d, 1H, $J = 2.4$ Hz), 7.58–7.61 (m, 3H), 7.26–7.31 (m, 2H), 4.47 (t, 2H, $J = 5.4$ Hz), 3.87 (t, 2H, $J = 5.4$ Hz). ^{13}C NMR (150 MHz, $\text{DMSO}-d_6$) δ 163.4, 154.1, 141.1, 137.2, 132.8, 132.0, 130.2, 129.3, 126.5, 126.2, 125.9, 125.0, 123.9, 115.5, 112.0, 69.1, 31.1. HRMS (ESI) calcd for $\text{C}_{17}\text{H}_{14}\text{BrClNO}_4\text{S}$ 441.9510 ($\text{M} + \text{H}^+$), found 441.9515.

4.1.2. 5-Chloro-N-(1,1-dioxo-1H-1 λ^6 -benzo[b]thiophen-6-yl)-2-(2-fluoroethoxy)benzamide (**3**)

Compound **3** was prepared in 77% yield by a procedure similar to that used to prepare compound **2**. The title compound was obtained as a pale yellow solid (mp 216–217 °C). ^1H NMR (600 MHz, $\text{DMSO}-d_6$) δ 10.63 (s, 1H), 8.21 (s, 1H), 7.85–7.86 (m, 1H), 7.68 (d, 1H, $J = 2.4$ Hz), 7.58–7.61 (m, 3H), 7.26–7.31 (m, 2H), 4.74–4.83 (m,

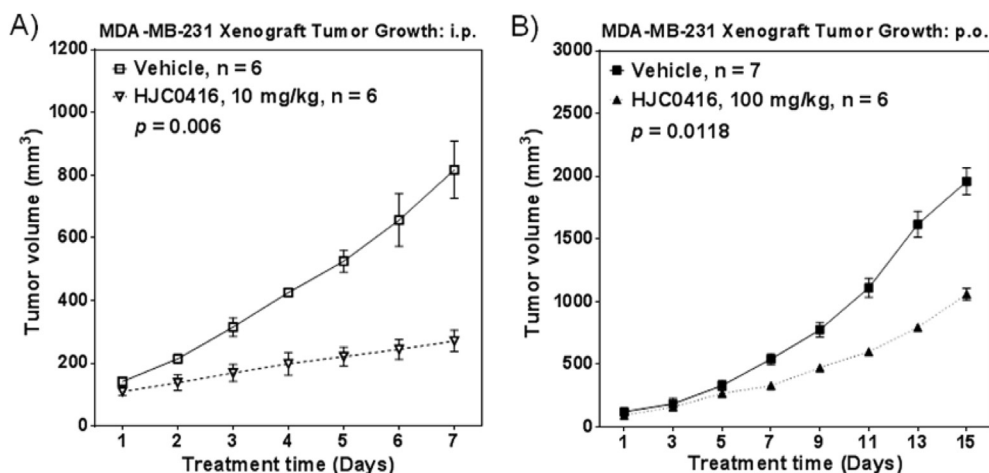


Fig. 6. In vivo efficacy of compound **12** (**HJC0416**) in inhibiting growth of xenograf tumors (triple-negative breast cancer MDA-MB-231) in mice via A) i.p. or B) oral gavage (p.o.) routes.

2H), 4.37–4.43 (m, 2H). ^{13}C NMR (150 MHz, DMSO- d_6) δ 163.6, 154.3, 141.1, 137.2, 132.8, 131.9, 130.2, 129.1, 126.6, 126.4, 125.9, 124.9, 123.7, 115.5, 111.7, 82.1 (d, $J = 166$ Hz), 68.5 (d, $J = 18$ Hz). HRMS (ESI) calcd for $\text{C}_{17}\text{H}_{14}\text{ClFN}_4\text{O}_4\text{S}$ 382.0311 ($\text{M} + \text{H}$) $^+$, found 382.0314.

4.1.3. 5-Chloro-*N*-(1,1-dioxo-1*H*-1 λ^6 -benzo[*b*]thiophen-6-yl)-2-(1-methylpiperidin-4-yl)oxy benzamide (**4**)

Compound **4** was prepared in 39% yield by a procedure similar to that used to prepare compound **2**. The title compound was obtained as a pale yellow solid (mp 220–221 °C). ^1H NMR (600 MHz, DMSO- d_6) δ 10.63 (s, 1H), 8.22 (s, 1H), 7.85 (d, 1H, $J = 7.2$ Hz), 7.58–7.61 (m, 3H), 7.51–7.53 (m, 1H), 7.27–7.30 (m, 2H), 4.53–4.55 (m, 1H), 2.42–2.44 (m, 2H), 2.19–2.21 (m, 2H), 2.06 (s, 3H), 1.89–1.91 (m, 2H), 1.69–1.71 (m, 2H). ^{13}C NMR (150 MHz, DMSO- d_6) δ 164.1, 153.2, 141.2, 137.2, 132.8, 131.5, 130.1, 128.8, 128.0, 126.6, 125.8, 124.4, 123.5, 116.8, 111.6, 79.2, 51.6, 45.8, 30.0. HRMS (ESI) calcd for $\text{C}_{21}\text{H}_{22}\text{ClN}_2\text{O}_4\text{S}$ 433.0983 ($\text{M} + \text{H}$) $^+$, found 433.0989.

4.1.4. 5-Chloro-2-(2-dimethylamino-ethoxy)-*N*-(1,1-dioxo-1*H*-1 λ^6 -benzo[*b*]thiophen-6-yl) benzamide (**5**)

Compound **5** was prepared in 62% yield by a procedure similar to that used to prepare compound **2**. The title compound was obtained as a pale yellow solid (mp 189–190 °C). ^1H NMR (600 MHz, CDCl_3) δ 10.77 (s, 1H), 8.41 (d, 1H, $J = 7.8$ Hz), 8.24 (d, 1H, $J = 1.8$ Hz), 7.99 (s, 1H), 7.43–7.45 (m, 1H), 7.33 (d, 1H, $J = 8.4$ Hz), 7.20 (d, 1H, $J = 6.6$ Hz), 6.97 (d, 1H, $J = 9.0$ Hz), 6.64 (d, 1H, $J = 7.2$ Hz), 4.26 (t, 2H, $J = 5.4$ Hz), 2.84 (t, 2H, $J = 4.2$ Hz), 2.39 (s, 6H). ^{13}C NMR (150 MHz, CDCl_3) δ 162.4, 155.3, 141.9, 137.6, 133.4, 132.5, 132.5, 129.7, 127.5, 126.0, 124.5, 123.0, 114.3, 66.1, 57.9, 45.2. HRMS (ESI) calcd for $\text{C}_{19}\text{H}_{20}\text{ClN}_2\text{O}_4\text{S}$ 407.0827 ($\text{M} + \text{H}$) $^+$, found 407.0831.

4.1.5. 5-Chloro-*N*-(1,1-dioxo-1*H*-1 λ^6 -benzo[*b*]thiophen-6-yl)-2-(2-morpholin-4-yl-ethoxy) benzamide (**6**)

Compound **6** was prepared in 67% yield by a procedure similar to that used to prepare compound **2**. The title compound was obtained as a white solid (mp 214–215 °C). ^1H NMR (600 MHz, DMSO- d_6) δ 10.72 (s, 1H), 8.18 (s, 1H), 7.90 (d, 1H, $J = 8.4$ Hz), 7.73 (d, 1H, $J = 2.4$ Hz), 7.58–7.62 (m, 3H), 7.27–7.32 (m, 2H), 4.26–4.28 (m, 2H), 3.43–3.45 (m, 4H), 2.74–2.76 (m, 2H), 2.42–2.50 (m, 4H). ^{13}C NMR (150 MHz, DMSO- d_6) δ 163.4, 154.8, 141.0, 137.2, 132.8, 132.1, 130.2, 129.2, 126.5, 126.0, 125.5, 124.7, 124.1, 115.4, 112.1, 66.7, 66.0, 56.6, 53.3. HRMS (ESI) calcd for $\text{C}_{21}\text{H}_{22}\text{ClN}_2\text{O}_5\text{S}$ 449.0932 ($\text{M} + \text{H}$) $^+$, found 449.0942.

4.1.6. 5-Chloro-*N*-(1,1-dioxo-1*H*-1 λ^6 -benzo[*b*]thiophen-6-yl)-2-(2-piperidin-1-yl-ethoxy) benzamide (**7**)

To a solution of **2** (50 mg, 0.11 mmol), KI (28 mg, 0.17 mmol) and K_2CO_3 (32 mg, 0.23 mmol) in acetone (5 mL) was added piperidine (49 mg, 0.57 mmol) at 0 °C. The mixture was stirred at 75 °C for 18 h. The solution was diluted with EtOAc (100 mL), washed with 0.1 N HCl (aq.) (10 mL) and brine (10 mL). The organic layer was dried over anhydrous Na_2SO_4 , and then concentrated under reduced pressure. The residue was purified by silica gel column chromatography (hexane/EtOAc = 1/1 to 1/3) to give the desired product **7** (50 mg, 98%) as a pale yellow solid (mp 180–181 °C). ^1H NMR (600 MHz, DMSO- d_6) δ 10.71 (s, 1H), 8.20 (s, 1H), 7.89 (d, 1H, $J = 7.8$ Hz), 7.74 (d, 1H, $J = 2.4$ Hz), 7.59–7.62 (m, 3H), 7.27–7.31 (m, 2H), 4.25 (t, 2H, $J = 5.4$ Hz), 2.70–2.72 (m, 2H), 2.38–2.40 (m, 4H), 1.35–1.38 (m, 4H), 1.22–1.24 (m, 2H). ^{13}C NMR (150 MHz, DMSO- d_6) δ 163.3, 155.0, 141.0, 137.2, 132.8, 132.2, 130.2, 129.3, 126.5, 126.0, 125.3, 124.7, 124.1, 115.4, 112.2, 66.9, 56.9, 54.1, 25.4, 23.8. HRMS (ESI) calcd for $\text{C}_{22}\text{H}_{24}\text{ClN}_2\text{O}_4\text{S}$ 447.1140 ($\text{M} + \text{H}$) $^+$, found 447.1145.

4.1.7. 5-Chloro-*N*-(1,1-dioxo-1*H*-1 λ^6 -benzo[*b*]thiophen-6-yl)-2-[2-(4-methylpiperazin-1-yl)-ethoxy] benzamide (**8**)

Compound **8** was prepared in 77% yield by a procedure similar to that used to prepare compound **7**. The title compound was obtained as a pale yellow solid (mp 218–219 °C). ^1H NMR (600 MHz, DMSO- d_6) δ 10.70 (s, 1H), 8.17 (s, 1H), 7.89–7.90 (m, 1H), 7.73 (d, 1H, $J = 3.0$ Hz), 7.58–7.62 (m, 3H), 7.26–7.31 (m, 2H), 4.25 (t, 2H, $J = 5.4$ Hz), 2.73 (t, 2H, $J = 4.8$ Hz), 2.42–2.50 (m, 4H), 2.12–2.22 (m, 4H), 2.03 (s, 3H). ^{13}C NMR (150 MHz, DMSO- d_6) δ 163.3, 154.9, 141.0, 137.2, 132.8, 132.2, 130.2, 129.2, 126.5, 126.0, 125.4, 124.7, 124.2, 115.4, 112.2, 66.9, 56.2, 54.5, 52.7, 45.6. HRMS (ESI) calcd for $\text{C}_{22}\text{H}_{25}\text{ClN}_3\text{O}_4\text{S}$ 462.1249 ($\text{M} + \text{H}$) $^+$, found 462.1253.

4.1.8. 5-Chloro-*N*-(1,1-dioxo-1*H*-1 λ^6 -benzo[*b*]thiophen-6-yl)-2-(2-piperazin-1-yl-ethoxy) benzamide (**9**)

To a solution of 5-chloro-*N*-(1,1-dioxo-1*H*-1 λ^6 -benzo[*b*]thiophen-6-yl)-2-hydroxybenzamide (100 mg, 0.3 mmol) and PPh₃ (157 mg, 0.6 mmol) in THF (5 mL) was added 4-(2-hydroxyethyl)-piperazine-1-carboxylic acid *tert*-butyl ester (138 mg, 0.6 mmol) in THF (5 mL) and DIAD (109 mg, 0.54 mmol). The mixture was stirred at r.t. for 2 h, and then was concentrated to give the crude product. This residue was purified with silica gel column (EtOAc/hexane = 1/1) to afford 80 mg of the intermediate as a pale yellow solid. To the solution of the intermediate (80 mg) in CH_2Cl_2 (5 mL) was added TFA (1 mL) at 0 °C. The mixture was stirred at r.t. for 3 h, and then was concentrated. The residue was partitioned between EtOAc (250 mL) and 1 N NaHCO_3 (10 mL). The organic layer was washed with H_2O (10 mL) and dried with Na_2SO_4 . The organic layer was concentrated. The residue was washed with EtOAc (10 mL) and then the solid was filtered to give **9** (65 mg, 48%, two steps) as a pale yellow solid (mp 206–207 °C). ^1H NMR (600 MHz, DMSO- d_6) δ 10.71 (s, 1H), 8.52 (s, 1H), 8.21 (s, 1H), 7.87–7.89 (m, 1H), 7.69 (d, 1H, $J = 2.4$ Hz), 7.58–7.63 (m, 3H), 7.32 (d, 1H, $J = 7.2$ Hz), 7.26 (d, 1H, $J = 8.4$ Hz), 4.24 (t, 2H, $J = 4.8$ Hz), 2.96 (t, 4H, $J = 4.8$ Hz), 2.82 (t, 2H, $J = 4.8$ Hz), 2.62–2.64 (m, 4H). ^{13}C NMR (150 MHz, DMSO- d_6) δ 163.6, 154.6, 141.1, 137.2, 132.9, 132.0, 130.2, 129.1, 126.6, 126.0, 126.0, 124.6, 123.8, 115.2, 111.9, 66.9, 55.8, 49.4, 42.9. HRMS (ESI) calcd for $\text{C}_{21}\text{H}_{23}\text{ClN}_3\text{O}_4\text{S}$ 448.1092 ($\text{M} + \text{H}$) $^+$, found 448.1101.

4.1.9. 5-Chloro-*N*-(1,1-dioxo-1*H*-1 λ^6 -benzo[*b*]thiophen-6-yl)-2-(piperidin-4-yl)oxy benzamide (**10**)

Compound **10** was prepared in 52% yield by a procedure similar to that used to prepare compound **9**. The title compound was obtained as a pale yellow solid (mp 128–129 °C). ^1H NMR (600 MHz, DMSO- d_6) δ 10.73 (s, 1H), 8.26 (s, 1H), 7.81–7.82 (m, 1H), 7.58–7.63 (m, 3H), 7.54–7.61 (m, 1H), 7.29–7.31 (m, 2H), 4.72–4.73 (m, 1H), 3.03–3.07 (m, 2H), 2.87–2.90 (m, 2H), 1.98–2.01 (m, 2H), 1.74–1.77 (m, 2H). ^{13}C NMR (150 MHz, DMSO- d_6) δ 164.2, 152.8, 141.3, 137.2, 132.9, 131.4, 130.2, 128.9, 128.2, 126.6, 125.9, 124.6, 123.6, 116.7, 111.6, 71.7, 41.1, 28.5. HRMS (ESI) calcd for $\text{C}_{20}\text{H}_{20}\text{ClN}_2\text{O}_4\text{S}$ 419.0827 ($\text{M} + \text{H}$) $^+$, found 419.0834.

4.1.10. 2-(2-Aminoethoxy)-5-chloro-*N*-(1,1-dioxo-1*H*-1 λ^6 -benzo[*b*]thiophen-6-yl) benzamide (**11**)

Compound **11** was prepared in 40% yield by a procedure similar to that used to prepare compound **9**. The title compound was obtained as a pale yellow solid (mp 202–203 °C). ^1H NMR (600 MHz, acetone- d_6) δ 10.85 (s, 1H), 8.19 (s, 1H), 8.13–8.15 (m, 1H), 8.06 (d, 1H, $J = 3.0$ Hz), 7.55–7.59 (m, 2H), 7.51–7.52 (m, 1H), 7.33 (d, 1H, $J = 8.4$ Hz), 6.99 (d, 1H, $J = 7.2$ Hz), 4.52 (t, 2H, $J = 4.8$ Hz), 3.80 (t, 2H, $J = 4.8$ Hz), 1.92–1.96 (m, 2H). ^{13}C NMR (150 MHz, DMSO- d_6) δ 163.4, 154.8, 141.2, 137.1, 132.6, 132.1, 130.1, 129.5, 126.4, 125.8, 125.8, 124.6, 124.1, 116.0, 112.1, 71.2, 40.4. HRMS (ESI) calcd for $\text{C}_{17}\text{H}_{16}\text{ClN}_2\text{O}_4\text{S}$ 379.0514 ($\text{M} + \text{H}$) $^+$, found 379.0520.

4.1.11. 2-(3-Aminopropoxy)-5-chloro-N-(1,1-dioxo-1H-1 λ^6 -benzo[b]thiophen-6-yl)benzamide (**12**)

Compound **12** was prepared in 51% yield by a procedure similar to that used to prepare compound **9**. The title compound was obtained as a pale yellow solid (mp 115–116 °C). ¹H NMR (600 MHz, DMSO-*d*₆) δ 10.76 (s, 1H), 8.31 (s, 1H), 7.78–7.80 (m, 1H), 7.75 (s, 2H), 7.57–7.64 (m, 4H), 7.31 (d, 1H, *J* = 6.6 Hz), 7.21 (d, 1H, *J* = 8.4 Hz), 4.18 (t, 2H, *J* = 6.0 Hz), 2.95 (t, 2H, *J* = 6.6 Hz), 2.00–2.02 (m, 2H). ¹³C NMR (150 MHz, DMSO-*d*₆) δ 164.3, 154.3, 141.3, 137.2, 132.8, 131.6, 130.2, 128.8, 126.8, 126.6, 125.9, 124.3, 123.8, 114.8, 111.8, 66.0, 36.5, 26.5. HRMS (ESI) calcd for C₁₈H₁₈ClN₂O₄S 393.0670 (M + H)⁺, found 393.0678.

4.1.12. 5-Chloro-N-(1,1-dioxo-1H-1 λ^6 -benzo[b]thiophen-6-yl)-2-(2-methylaminoethoxy)benzamide (**13**)

Compound **13** was prepared in 43% yield by a procedure similar to that used to prepare compound **9**. The title compound was obtained as a white solid (mp 175–176 °C). ¹H NMR (600 MHz, CDCl₃) δ 10.77 (s, 1H), 8.36–8.38 (m, 1H), 8.21 (d, 1H, *J* = 2.4 Hz), 8.10 (s, 1H), 7.44–7.46 (m, 1H), 7.35 (d, 1H, *J* = 8.4 Hz), 7.21–7.22 (m, 1H), 6.98 (d, 1H, *J* = 9.0 Hz), 6.67 (d, 1H, *J* = 6.6 Hz), 4.31 (t, 2H, *J* = 4.8 Hz), 3.18 (t, 2H, *J* = 5.4 Hz), 2.64 (s, 3H). ¹³C NMR (150 MHz, CDCl₃) δ 162.6, 155.2, 141.8, 137.6, 133.3, 132.5, 132.4, 129.6, 127.4, 126.0, 124.5, 123.3, 114.3, 114.1, 68.3, 50.8, 36.5. HRMS (ESI) calcd for C₁₈H₁₈ClN₂O₄S 393.0670 (M + H)⁺, found 393.0678.

4.1.13. 5-Chloro-N-(3-methoxy-1,1-dioxo-2,3-dihydro-1H-1 λ^6 -benzo[b]thiophen-6-yl)-2-hydroxybenzamide (**14**)

To the solution of 5-chloro-N-(1,1-dioxo-1H-1 λ^6 -benzo[b]thiophen-6-yl)-2-hydroxybenzamide (335 mg, 1.0 mmol) in MeOH (8 mL) was added 10% NaOH (2 mL, 5.0 mmol) at 0 °C. The mixture was stirred at r.t. for 15 min. The mixture was diluted with EtOAc (100 mL) and washed with 2 N HCl (20 mL) and brine (20 mL). The organic layer was separated and dried with anhydrous Na₂SO₄. The solution was concentrated to afford the crude product, which was washed with CH₂Cl₂ (5 mL) to give the desired product (220 mg, 60%) as a pale yellow solid (mp 268–269 °C). ¹H NMR (600 MHz, DMSO-*d*₆) δ 11.52 (s, 1H), 10.73 (s, 1H), 8.24 (s, 1H), 7.95 (d, 1H, *J* = 8.4 Hz), 7.88 (s, 1H), 7.70 (d, 1H, *J* = 9.0 Hz), 7.49 (d, 1H, *J* = 9.0 Hz), 7.03 (d, 1H, *J* = 8.4 Hz), 5.17–5.18 (m, 1H), 3.96–3.99 (m, 1H), 3.65–3.67 (dd, 1H, *J* = 3.0, 13.8 Hz), 3.40 (s, 3H). ¹³C NMR (150 MHz, DMSO-*d*₆) δ 165.2, 156.3, 140.5, 139.8, 133.1, 132.7, 128.6, 128.3, 125.7, 122.8, 120.2, 119.0, 111.1, 74.5, 56.8, 56.0. HRMS (ESI) calcd for C₁₆H₁₅ClNO₅S 368.0354 (M + H)⁺, found 368.0357.

4.2. Biology

4.2.1. In vitro determination of effects of synthesized compounds on cancer cell proliferation

Cancer cells (breast cancer cell lines MCF-7 and MDA-MB-231, pancreatic cancer cell lines AsPC-1 and Panc-1) were seeded in 96-well plates at a density of 2 × 10³ cells/well and treated with DMSO, 0.01, 0.1, 1, 5, 10, and 100 μ M of individual STAT3 inhibitors for 72 h. Proliferation was measured by treating cells with the 3-(4,5-dimethylthiazol-2-yl)-5-(3-carboxymethoxyphenyl)-2-((4-sulfophenyl)-2H-tetrazolium) (MTS) in a CellTiter 96 Aqueous Non-Radioactive Cell Proliferation Assay kit (Promega, Madison, WI, USA). Absorbance of all wells was determined by measuring OD at 550 nm after 1 h incubation at 37 °C on a 96-well iMark™ Microplate Absorbance Reader (BioRad, Hercules, CA). Each individual compound was tested in quadruplicate wells for each concentration.

4.2.2. Transient transfection and dual luciferase reporter assays

MDA-MB-231 cells were pre-treated with statin or **12** at 5 μ M for 24 h. Then the cells were trypsinized and seeded in 24-well plate at a density of 5 × 10⁴ cells/well in RPMI-1640 medium containing 10% FBS and 1% penicillin-streptomycin. Transient transfections were performed 4 h after plating, using the previously described method [18,24]. Total amount of DNA for transfections was 0.5 μ g/well, including pSTAT3-Luc (95%, obtained from Panomics, Cat# LR0077) and internal control vector renilla (5%, from Promega, Madison, WI, USA). 5 h after transfection, the cells were treated with statin or compound **12** for 24 h, and then reporter activity was evaluated using dual luciferase reporter assay kit (Promega, Madison, WI, USA) on an Omega™ Microplate Luminometer (BMG LABTECH Inc., NC, USA). Relative luciferase units were the ratio of the absolute activity of firefly luciferase to that of renilla luciferase. Experiments were conducted in triplicates and results are representatives of at least 3 independent experiments.

4.2.3. Molecular docking studies

Lead compound **1** and compound **12** were docked with the STAT3-SH2 domain (PDB code: 1BG1) [25] and AutoDock Vina 1.1.2, using the method as previously described [18,26,27]. Water molecules within the crystal structure were removed and polar hydrogens were added using AutoDockTools. The protein was treated as rigid. Docking runs were carried out using the standard parameters of the program for interactive growing and subsequent scoring, except for the parameters for setting grid box dimensions and center. For all of the docking studies, a grid box size of 30 Å × 30 Å × 30 Å, centered at coordinates 100.452 (x), 75.972 (y), and 68.790 (z) of the PDB structure.

4.2.4. Western blot analysis

Protein levels were determined by Western blot using the previously reported methods [18,24]. Total cell lysates were prepared from MDA-MB-231 cells. Protein concentrations were measured using the BCA Protein Assay Reagent (Pierce, Rockford, IL, USA). Equal amounts of total cellular protein extract (40 μ g) were resuspended in denaturing sample loading buffer (0.5 M Tris-HCl, pH 6.8, 10% SDS, 0.1% bromophenol blue, and 20% glycerol), separated by electrophoresis on a 10% polyacrylamide SDS-PAGE gel and then electrophoretically transferred to a nitrocellulose membrane (Thermo Scientific, IL, USA) at 100 V for 1 h at 4 °C. The membrane was then incubated in a blocking solution containing 5% non-fat milk and 1% Tween 20 in TBS for 1 h. The membrane was then incubated with antibodies specific for: phospho-STAT3-PY705 (1:3000, Epitomics, #2236-1), STAT3 (1:2000, Cell Signaling, #4904), Caspase-3-active (1:2000, Epitomics, #1476-1), Cyclin D1 (1:10,000, Epitomics, #2261-1) and β -actin (1:10,000, Sigma, clone AC-15). An anti-rabbit or anti-mouse secondary antibody (Amersham, Piscataway, NJ) was used at 1:4000 dilution. The Western blotted bands were visualized using ECL procedure according to the manufacturer's instructions (Amersham).

4.2.5. In vivo antitumor activity assays

All procedures including mice and *in vivo* experiments were approved by the Institutional Animal Care and Use Committee (IACUC) of UT M.D. Anderson Cancer Center (MDACC). Thirty-one female nude mice were obtained from MDACC and were used for orthotopic tumor studies at 6 weeks of age. The mice were maintained in a barrier unit with 12 h light–dark switch. Freshly harvested MDA-MB-231 cells (2.5 × 10⁶ cells per mouse, resuspended in 100 μ L PBS) were injected into the 3rd mammary fat pad of the mice, and then randomly assigned into 5 groups (5–10 mice per group). For the intraperitoneal treatment experiment, the mice were treated daily with 10 mg/kg of compound **12** (**HJC0416**), or

vehicle when the tumor volume reached 150 mm³. Similarly, for the oral gavage experiment, the mice were given 100 mg/kg of **12**, or vehicle five days per week when the tumor volume reached 110 mm³. All drugs were dissolved in 50% DMSO with 50% polyethylene glycol for *in vivo* administration. Body weights and tumors volume were measured daily and tumor volume was calculated according to the formula $V = 0.5 \times L \times W^2$, where L = length (mm) and W = width (mm).

4.2.6. Statistical analysis

Statistical significance was determined using student *t*-test in cell cycle analysis. * represents a *p* value less than 0.05.

Conflict of interest

The authors declare no competing financial interest.

Acknowledgments

This work was supported by grants P50 CA097007, P30 DA028821, R21 MH093844 (JZ) from the National Institutes of Health, a grant from Duncan Family Institute Seed Funding Research Program and a startup fund from MD Anderson Cancer Center (QS), R. A. Welch Foundation Chemistry and Biology Collaborative Grant from the Gulf Coast Consortia (GCC), a training fellowship from the Keck Center for Interdisciplinary Bioscience Training of the GCC (NIGMS grant T32 GM089657-03), Sealy and Smith Foundation grant (to the Sealy Center for Structural Biology and Molecular Biophysics), John Sealy Memorial Endowment Fund, and the Center for Addiction Research (CAR) at UTMB. We thank Drs. Lawrence C. Sowers, Jacob A. Theruvathu, and Tianzhi Wang for the NMR spectroscopy assistance, as well as Drs. Huiling Liu and Carol Nilsson for mass spectrometry assistance.

Appendix A. Supplementary data

Supplementary data related to this article can be found at <http://dx.doi.org/10.1016/j.ejmech.2014.05.049>.

References

- [1] J.E. Darnell Jr., STATs and gene regulation, *Science* 277 (1997) 1630–1635.
- [2] T. Bowman, R. Garcia, J. Turkson, R. Jove, STATs in oncogenesis, *Oncogene* 19 (2000) 2474–2488.
- [3] J. Bromberg, J.E. Darnell Jr., The role of STATs in transcriptional control and their impact on cellular function, *Oncogene* 19 (2000) 2468–2473.
- [4] J. Turkson, R. Jove, STAT proteins: novel molecular targets for cancer drug discovery, *Oncogene* 19 (2000) 6613–6626.
- [5] J. Bromberg, Stat proteins and oncogenesis, *J. Clin. Invest* 109 (2002) 1139–1142.
- [6] H. Yu, D. Pardoll, R. Jove, STATs in cancer inflammation and immunity: a leading role for STAT3, *Nat. Rev. Cancer* 9 (2009) 798–809.
- [7] P. Yue, J. Turkson, Targeting STAT3 in cancer: how successful are we? *Expert Opin. Investig. Drugs* 18 (2009) 45–56.
- [8] S. Haftchenary, M. Avadisian, P.T. Gunning, Inhibiting aberrant Stat3 function with molecular therapeutics: a progress report, *Anticancer Drugs* 22 (2011) 115–127.
- [9] R. Buettner, L.B. Mora, R. Jove, Activated STAT signaling in human tumors provides novel molecular targets for therapeutic intervention, *Clin. Cancer Res.* 8 (2002) 945–954.
- [10] J.F. Bromberg, M.H. Wrzeszczynska, G. Devgan, Y. Zhao, R.G. Pestell, C. Albanese, J.E. Darnell Jr., Stat3 as an oncogene, *Cell* 98 (1999) 295–303.
- [11] H. Yu, R. Jove, The STATs of cancer—new molecular targets come of age, *Nat. Rev. Cancer* 4 (2004) 97–105.
- [12] J.E. Darnell, Validating Stat3 in cancer therapy, *Nat. Med.* 11 (2005) 595–596.
- [13] B. Debnath, S. Xu, N. Neamati, Small molecule inhibitors of signal transducer and activator of transcription 3 (Stat3) protein, *J. Med. Chem.* 55 (2012) 6645–6668.
- [14] J. Deng, F. Grande, N. Neamati, Small molecule inhibitors of Stat3 signaling pathway, *Curr. Cancer Drug Targ.* 7 (2007) 91–107.
- [15] K. Al Zaid Siddiquee, J. Turkson, STAT3 as a target for inducing apoptosis in solid and hematological tumors, *Cell Res.* 18 (2008) 254–267.
- [16] B.D. Page, D.P. Ball, P.T. Gunning, Signal transducer and activator of transcription 3 inhibitors: a patent review, *Expert Opin. Ther. Pat.* 21 (2011) 65–83.
- [17] M.M. Hann, G.M. Keseru, Finding the sweet spot: the role of nature and nurture in medicinal chemistry, *Nat. Rev. Drug. Discov.* 11 (2012) 355–365.
- [18] H. Chen, Z. Yang, C. Ding, L. Chu, Y. Zhang, K. Terry, H. Liu, Q. Shen, J. Zhou, Fragment-based drug design and identification of HJC0123, a novel orally bioavailable STAT3 inhibitor for cancer therapy, *Eur. J. Med. Chem.* 62 (2013) 498–507.
- [19] H. Chen, Z. Yang, C. Ding, L. Chu, Y. Zhang, K. Terry, H. Liu, Q. Shen, J. Zhou, Discovery of -Alkylamino tethered niclosamide derivatives as potent and orally bioavailable anticancer agents, *ACS Med. Chem. Lett.* 4 (2013) 180–185.
- [20] A. Innocenti, R. Villar, V. Martinez-Merino, M.J. Gil, A. Scozzafava, D. Vullo, C.T. Supuran, Carbonic anhydrase inhibitors: inhibition of cytosolic/tumor-associated carbonic anhydrase isozymes I, II, and IX with benzo[b]thiophene 1,1-dioxide sulfonamides, *Bioorg. Med. Chem. Lett.* 15 (2005) 4872–4876.
- [21] D. Tang, E.T. McKinley, M.R. Hight, M.I. Uddin, J.M. Harp, A. Fu, M.L. Nickels, J.R. Buck, H.C. Manning, Synthesis and structure-activity relationships of 5,6,7-substituted pyrazolopyrimidines: discovery of a novel TSPO PET ligand for cancer imaging, *J. Med. Chem.* 56 (2013) 3429–3433.
- [22] J. Schust, B. Sperl, A. Hollis, T.U. Mayer, T. Berg, Stattic: a small-molecule inhibitor of STAT3 activation and dimerization, *Chem. Biol.* 13 (2006) 1235–1242.
- [23] O. Trott, A.J. Olson, AutoDock Vina: improving the speed and accuracy of docking with a new scoring function, efficient optimization, and multi-threading, *J. Comput. Chem.* 31 (2010) 455–461.
- [24] Q. Shen, I.P. Uray, Y. Li, T.I. Krisko, T.E. Strecker, H.T. Kim, P.H. Brown, The AP-1 transcription factor regulates breast cancer cell growth via cyclins and E2F factors, *Oncogene* 27 (2008) 366–377.
- [25] S. Becker, B. Groner, C.W. Muller, Three-dimensional structure of the Stat3-beta homodimer bound to DNA, *Nature* 394 (1998) 145–151.
- [26] H. Chen, T. Tsalkova, F.C. Mei, Y. Hu, X. Cheng, J. Zhou, 5-Cyano-6-oxo-1,6-dihydro-pyrimidines as potent antagonists targeting exchange proteins directly activated by cAMP, *Bioorg. Med. Chem. Lett.* 22 (2012) 4038–4043.
- [27] H. Chen, C.Z. Wang, C. Ding, C. Wild, B. Copits, G.T. Swanson, K.M. Johnson, J. Zhou, A combined bioinformatics and cheminformatics approach for developing asymmetric bivalent AMPA receptor positive allosteric modulators as neuroprotective agents, *ChemMedChem* 8 (2013) 226–230.